Substitutions in the Pheromone-Responsive G_β Protein of *Saccharomyces cerevisiae* Confer a Defect in Recovery from Pheromone Treatment

E Li,* Eric Meldrum,†,[1] Holly F. Stratton* and David E. Stone*

**Laboratory for Molecular Biology, University of Illinois at Chicago, Chicago, Illinois 60607 and †Department of Molecular Biology, The Scripps Research Institute, La Jolla, California 92037*

Manuscript received April 1, 1997
Accepted for publication November 21, 1997

ABSTRACT

The pheromone-responsive G_α protein of *Saccharomyces cerevisiae*, Gpa1p, stimulates an adaptive mechanism that downregulates the mating signal. In a genetic screen designed to identify signaling elements required for Gpa1p-mediated adaptation, a large collection of adaptive-defective (Adp^-) mutants were recovered. Of the 49 mutants characterized thus far, approximately three-quarters exhibit a dominant defect in the negative regulation of the pheromone response. Eight of the dominant Adp^- mutations showed tight linkage to the gene encoding the pheromone-responsive G_β, *STE4*. Sequence analysis of the *STE4* locus in the relevant mutant strains revealed seven novel *STE4* alleles, each of which was shown to disrupt proper regulation of the pheromone response. Although the *STE4* mutations had only minor effects on basal mating pathway activity, the mutant forms of G_β dramatically affected the ability of the cell to turn off the mating response after exposure to pheromone. Moreover, the signaling activity of the aberrant $G_{\beta\gamma}$ subunits was suppressed by G322E, a mutant form of Gpa1p that blocks the pheromone response by sequestering $G_{\beta\gamma}$, but not by E364K, a hyperadaptive form of Gpa1p. On the basis of these observations, we propose that Gpa1p-mediated adaptation involves the binding of an unknown negative regulator to $G_{\beta\gamma}$.

THE differentiation of proliferating haploid yeast cells into mating competent cells is triggered by the exchange of peptide-mating pheromones. Each of the two yeast mating types, *MAT***a** and *MAT*α, expresses a seven-transmembrane domain receptor that binds the pheromone secreted by cells of the opposite type. By analogy to mammalian systems, the pheromone-bound receptor is thought to activate its associated G protein by catalyzing the exchange of GTP for GDP on G_α, the result of which is a conformational shift in G_α and subsequent release of $G_{\beta\gamma}$. The signal is then transmitted by $G_{\beta\gamma}$ to a MAP kinase cascade, ultimately resulting in the activation of a mating-specific transcription factor and the degradation of G_1 cyclins (for reviews see Kurjan 1992; Sprague and Thorner 1992). Thus, haploid yeast cells arrest in the G_1 phase of the cell cycle, induce mating-specific genes, and elongate toward their mating partners in preparation for cytoplasmic and nuclear fusion.

The basal activity of the pheromone signaling pathway and the duration of the response after stimulus are regulated in numerous ways. The known negative regulatory mechanisms involve both types of pheromones (MacKay *et al.* 1988; Marcus *et al.* 1991) and their receptors (Konopka *et al.* 1988; Reneke *et al.* 1988), the G protein (Cole and Reed 1991; Stratton *et al.* 1996), and one of the MAP kinases (Doi *et al.* 1994). These apparently redundant mechanisms may serve distinct purposes, such as promoting desensitization to a chronic stimulus, rapidly terminating the pheromone response upon diploid formation, and balancing sensitivity to pheromone against inappropriate induction of the mating signal. The need for complex and subtle modulation of this signaling pathway may be satisfied in part by the pheromone-responsive G_α protein Gpa1p. Gpa1p has been postulated to oppose the activity of its βγ subunit (encoded by *STE4* and *STE18*) in at least two ways. In what is presumed to be its inactive (GDP-bound) state, Gpa1p sequesters $G_{\beta\gamma}$. In what is presumed to be its active (GTP-bound) form, Gpa1p stimulates an adaptive mechanism that is independent of $G_{\beta\gamma}$ sequestration (Stratton *et al.* 1996). Whether Gpa1p inhibits the mating signal by direct interaction with $G_{\beta\gamma}$ or by indirect means presumably depends on the degree to which the receptor is stimulated, as well as on other unknown factors.

It has recently become clear that yeast is not exceptional in its use of $G_{\beta\gamma}$ as a signaling molecule. $G_{\beta\gamma}$ dimers are now known to interact with effector mole-

Corresponding author: David Stone, Laboratory for Molecular Biology (M/C 567), Department of Biological Sciences, University of Illinois at Chicago, 900 South Ashland Avenue, Chicago, IL 60607.
E-mail: U62248@uicvm.uic.edu

[1] *Present address:* Glaxo Institute for Molecular Biology S. A., 14, chemin des Auix—Case Postale 674, 1228 Plan-les-Quates, Geneva, Switzerland.

cules and induce signals in many systems (Clapham and Neer 1993; Iniguez-Lluhi *et al.* 1993). How the signaling activity of $G_{\beta\gamma}$ is controlled and how the signals generated by a given G_α and its $\beta\gamma$ are related are, therefore, questions of increasing interest. In yeast, the relationship between G_α and $G_{\beta\gamma}$ is clearly antagonistic. Pheromone–receptor binding results in a bifurcated signal: the heterotrimeric G protein separates into its two functional subunits and free $G_{\beta\gamma}$ induces changes in cellular physiology that are, after a delay, counteracted by activated G_α. An analogous antagonism between activated G_α and free $G_{\beta\gamma}$ has recently been found in three metazoan systems (Crespo *et al.* 1995; Liu and Simon 1996; Schreibmayer *et al.* 1996).

In an effort to better understand how G protein signals are regulated and, specifically, to identify downstream components in the Gpa1p-mediated adaptive pathway, we undertook a screen for genomic mutations that result in supersensitive/adaptive defects. Here we describe the characterization of seven novel alleles of *STE4* (G_β), all of which confer a dominant Adp^- phenotype. We show that although some of these mutant forms of G_β have little effect on basal signaling, they dramatically compromise the ability of the cell to recover from pheromone treatment. Our data also suggest that contrary to previous conclusions, Gpa1p-mediated adaptation does not stimulate Ste4p phosphorylation (Cole and Reed 1991). In fact, our results suggest that the phosphorylation of Ste4p plays no role in adaptation.

MATERIALS AND METHODS

Yeast strains, media, and microbiological techniques: Yeast growth media were prepared as described by Sherman *et al.* (1986). Tryptophan, adenine, histidine, and uracil were omitted from synthetic media as necessary to maintain plasmids or select diploids. For experiments requiring the induction of the *GAL1*-regulated genes, cells were grown to midlog phase in selective sucrose medium, and galactose was added to a final concentration of 2%, or the cells were pelleted and resuspended in selective galactose medium. Yeast transformations were carried out according to the method of Ito *et al.* (1983).

All strains constructed for this study were derived from strain 15Dau *bar1*Δ (*MAT***a** *bar1*Δ *ade1 his2 leu2-3,-112 trp1 ura3*Δ), which is congenic with strain BF264-15D, as described previously (Reed *et al.* 1985). Unless otherwise noted, the designation of cells as wild type, *GPA1-E364K*, or *GPA1-G322E* refers to strain 15Dau *bar1*Δ transformed with the centromeric vectors YCplac22 or YCplac33 (Gietz and Sugino 1988) containing the wild-type, E364K, or G322E alleles of *GPA1*, respectively (Stone and Reed 1990). Thus, these strains express a plasmid-borne allele of *GPA1* as well as the native copy of *GPA1*.

The parent strain for the mutant hunt, DSY278, was created by sequentially integrating the P_{GAL1}-*GPA1-E364K* (previously denoted $GAL1^{EG28}$-E364K in Stratton *et al.* 1996) and *FUS1-LEU2* constructs at the *TRP1* and *HIS2* loci, respectively, and then transforming the resulting strain with the *GAL1-CLN3-2* centromeric vector YCp50/*GAL1-CLN3-2* (Cross 1988).

The *ste4*Δ*::LEU2* deletion strain ELY100, which was used in the linkage analysis and for the measurement of growth rates, was created by integrating the *FUS1-LEU2* construct at the *HIS2* locus and transplacing the wild-type *STE4* allele with a *ste4*Δ*::LEU2* deletion/disruption construct.

To assess the effects of the adaptive-defective *STE4* (*STE4* Adp^-) alleles in a clean genetic background, the wild-type *STE4* allele was replaced by the various mutant alleles in a two-step process. The *ste4*Δ*::URA3* sequence was excised as a 4.0-kb *Eco*RI-*Sph*I fragment from the *ste4*Δ*::URA3*/YCplac33 plasmid, gel purified, and used to transform strain 15Dau *bar1*Δ. Disruption and deletion of the chromosomal *STE4* locus was confirmed by PCR analysis and mating assays, and the resulting strain was named ELY104. To replace the chromosomal *ste4*Δ*::URA3* construct with the various *STE4* Adp^- alleles, the mutant *STE4* sequences were excised as 3.4-kb *Eco*RI-*Sph*I fragments from the various YCplac33/*STE4* plasmids and were transformed into strain ELY104. Transformants were selected by growth on medium containing 5-fluoroorotic acid (FOA), which counterselects the *URA3* marker. All gene replacements were confirmed by PCR analysis and halo tests.

Plasmids: Recombinant DNA techniques were essentially as described by Sambrook *et al.* (1989) and Ausubel *et al.* (1994). Plasmids created for this study were constructed as follows:

YCplac33/$STE4^{\Delta Hd}$: Plasmid YCplac33/*STE4* (provided by Dr. G. Cole) contains three *Hin*dIII sites, two in the coding region of *STE4* and one in the polylinker. This plasmid was partially digested with *Hin*dIII, and the ends were reclosed by treatment with Klenow and T4 ligase. The desired clone, a YCplac33/*STE4* plasmid lacking only the target *Hin*dIII site, was isolated by screening bacterial transformants. Digestion of this plasmid (YCplac33/$STE4^{\Delta Hd}$) with *Hin*dIII deletes the sequence encoding residues 63–398 of Ste4p.

ste4Δ::URA3*/YCplac33:* The sequence encoding residues 63–398 of Ste4p in YCplac33/*STE4* was replaced by a *Hin*dIII fragment containing the *URA3* gene.

YCplac33/GPA1-E364K, *YCplac33*/GPA1-G322E, *and YCplac33*/GPA1*:* The *Xba*I-*Sac*I fragment containing the coding region of *GPA1* and 1.75 kb of the 5′ flanking sequence was moved from YCplac111 plasmids containing *GPA1-E364K*, *GPA1-G322E*, and wild-type *GPA1* (Stone and Reed 1990) to YCplac33 (Gietz and Sugino 1988).

FUS1-lacZ::ADE1*:* The *ADE1* gene was amplified by PCR using PUC19-*ADE1*(-B) (provided by Dr. P. Hagley) as the template and Pfu (Stratagene, La Jolla, CA) as the thermophilic polymerase. The product was then ligated to the TA cloning vector pCRII (Invitrogen, San Diego, CA) to yield pCRII/*ADE1*. The fragment containing *ADE1* was isolated from pCRII/*ADE1* by digestion with *Apa*I, followed by gel purification and ligation to *Apa*1 cut and phosphatased pSB231 (Trueheart *et al.* 1987), thereby disrupting the *URA3* gene.

Pheromone response and growth assays: Strains were tested for pheromone-induced growth inhibition in standard halo assays, as described previously (Cole *et al.* 1990). After growth to midlog phase, $\sim 10^5$ cells were diluted into 7 ml top agar (0.7%) and spread onto plates. Four-microgram doses of synthetic α factor (Multiple Peptide Systems, San Diego, CA) were then dotted onto the surface of the plates in 4-microliter aliquots. The plates were incubated for 2 days at 30° before photographing.

For determination of growth rates (Table 1), the *STE4* wild-type and mutant transplacement strains were grown to midlog phase in rich medium (YEPD) at 30°, and the A_{600} of each culture was measured over three doublings. Throughout the experiment, the cells were maintained in exponential growth by periodic dilution with warm medium.

Immunoblots: Crude cell lysates were prepared as follows: 2×10^8 midlog cells were harvested and boiled in 200 μg of 2× sample buffer [0.24 m Tris-HCl (pH 6.8), 2% SDS, 2% β-mercaptoethanol, 20% glycerol] for 4 min. Acid-washed glass beads (0.45 mm) were added to the suspension, and the mix-

TABLE 1

Phenotypes conferred by dominant Adp$^-$ *STE4* alleles

Mutant strain	Substitution	Growth rate[d]	Δ growth rate[f]	Halo size (cm)	
				GPA1	*GPA1-E364K*
Wild-type *STE4*	—	105 ± 9	—	3.0	—
A34[a]	F115S	139 ± 25	32.4	3.6	3.6; light fill
A27[a]	L138F	113 ± 4	7.6	3.2	3.3; light fill
A35[a]	A405V	106 ± 10	1.0	3.4	3.1; light fill
A37[a]	G409D	109 ± 16	3.8	3.3	3.1; light fill
A6[c], A39[b], B22[b]	S410L	111 ± 21	5.7	3.3	3.0; light fill
A12[a]	W411L	108 ± 7	2.9	3.3	2.5; light fill
A44[b]	W411S	ND[e]	—	3.3	2.8; light fill

[a] Alleles recovered by gap repair and sequenced in their entirety.
[b] Alleles recovered by PCR and sequenced in the C-terminal region (from the codon corresponding to residue 380 to the end of the gene).
[c] Alleles recovered from a genomic library and sequenced in their entirety.
[d] The mean doubling time in minutes derived from three independent experiments ± 1 SD.
[e] Not determined.
[f] Percent increase in doubling time.

ture was vortexed vigorously at 4° until lysis was complete and then boiled again for 2 min. The lysates were spun at 2000 rpm to remove the glass beads and then for 10 min at 12,000 *g* to pellet the cell debris. The resulting lysates were normalized by measuring absorbance at 280 nm. Samples containing ~0.4 A_{280} unit were electrophoresed on a discontinuous SDS-polyacrylamide gel (4%/10%) and electroblotted to PVDF-Plus transfer membrane (Micron Separations, Inc., Westboro, MA) according to the protocol supplied with the semidry blotter (Fisher Scientific, Pittsburgh, PA). Blots were then blocked with 5% nonfat dry milk in TBS overnight. The blots were subsequently incubated with diluted, strip-purified antisera raised against full-length Ste4p (45) in 0.2× blocking solution in TBS for 4 hr, and then processed with the ECL immunoblot detection kit (Amersham, Arlington Heights, IL) according to the manufacturer's instructions. Strip purification of the Ste4p antisera was performed according to the method described by Harlow and Lane (1988) using GST-Ste4p fusion protein purified from *Escherichia coli*.

Genetic screen and characterization: *Mutant selection:* 2 × 10^7 cells of strain DSY278 were spread on YEPD plates and mutagenized with UV radiation to 50% lethality by inverting the plates for ~3 sec on a short-wave UV transilluminator. After incubation in the dark for 3 days, the cells were replica-plated to synthetic sucrose medium lacking uracil, incubated for an additional 2 days, and then replica plated to the selection media (synthetic galactose medium containing 20 ng, 0.5 μg, or 2 μg α factor and lacking leucine). After 3 days of growth, colonies of all sizes were streaked onto fresh selection plates containing the same amount of α factor (20 ng, 0.5 μg, or 2 μg), and were allowed to grow for an additional 2 days. The mutants were then grown on rich medium lacking pheromone for 2 days before being tested for growth on synthetic glucose medium lacking leucine and on YEPD plates containing 10, 25, 50, 75, 100, and 125 ng of α factor. Finally, the putative mutants were scored for leucine prototrophy and projection formation on medium lacking α factor. All incubations were at 30°.

Backcrosses: Putative Adp$^-$ mutants were crossed to 15Dau *bar1*Δ carrying YCplac33 (Gietz and Sugino 1988), and the mating mixtures were spread onto synthetic galactose medium lacking histidine, uracil, and tryptophan (SG-HUT) to select diploids. After sporulation on potassium acetate plates, asci were dissected or subjected to random spore analysis.

Dominance test: All mutants to be tested for dominance were crossed to a *MAT***a** deletion strain, (KT23αx8:EG123: *ura3 leu2 trp1 his4 BAR1*; Tatchell *et al.* 1981), transformed with pJM9, a YCp50-based plasmid carrying the *MAT*α locus (provided by Hay-Oak Park), and mated on rich galactose-containing medium (YEPG) for 8 hr at 30°. Diploids were then selected from the mating mixture by sequentially spreading onto SG-HUT plates twice. The resulting diploid cells were grown overnight on rich medium at 30° before being replica plated to medium containing galactose and 0.5 μg/ml FOA. Ura$^-$ cells were picked from FOA-resistant patches, uracil auxotrophy was confirmed, and halo tests were performed on YEPD and YEPG.

Linkage analysis: The Adp$^-$ mutant strains were tested for linkage to *STE4* as follows: The mutant strains were crossed to strain ELY100, which is a *MAT*α *ste4*Δ*::LEU2 FUS1-LEU2* strain isogenic with the parent strain, DSY278. Diploid cells were sporulated, asci were dissected, and segregants were scored for leucine prototrophy. At least 12 asci were dissected for each mutant strain. Mutations linked to *STE4* were expected to segregate 4 Leu$^+$:0 Leu$^-$.

Gap repair: Mutant *STE4* alleles were retrieved from their genomic loci by gap repair (Orr-Weaver *et al.* 1983; Rothstein 1991). YCplac33/*STE4*$^{\Delta Hd}$ was digested with *Hin*dIII and *Xho*I, which removes the sequence-encoding residues 63–398 of Ste4p, gel purified, and used to transform the various *STE4* mutant strains. Ura$^+$ transformants were selected. Plasmids recovered from these yeast transformants were amplified in *E. coli* and were used to transform the parent strain DSY278. Plasmids that caused DSY278 cells to exhibit a defect in recovery from pheromone treatment were subjected to sequence analysis.

Sequence analysis: Dideoxy sequence reactions were performed using the Sequenase Version 2.0 kit (United States Biochemical, Cleveland, OH).

Measurement of FUS1-lacZ activity: *FUS1* promoter activity was assayed in cells transformed with a centromeric reporter plasmid, *FUS1-lacZ::ADE1*, derived from pSB231 (Trueheart *et al.* 1987). β-galactosidase activity was measured as described previously (Slater and Craig 1987).

RESULTS

Isolation of Adp$^-$ mutants: As a first step toward understanding how the activated form of Gpa1p promotes adaptation, we sought genomic mutations that would disrupt the ability of E364K, a hyperadaptive allele of *GPA1*, to confer resistance to pheromone. To create a strain in which viability would depend on such a mutation, three constructs were introduced into the *MAT***a** *leu2-3,-112* strain 15Dau: *FUS1-LEU2*, P_{GAL1}-GPA1-E364K, and *GAL1-CLN3-2*. Our rationale for the construction of this strain, DSY278, was as follows: The hybrid gene composed of the pheromone-inducible *FUS1* promoter fused to the coding region of *LEU2* allows the parent strain to grow in leucine-deficient media if the pheromone signaling pathway is activated. Activation of the pathway does not inhibit growth because the *CLN3-2* allele, a dominant mutation that stabilizes one of the G_1 cyclins in yeast, uncouples pheromone-induced transcription from pheromone-induced G_1 arrest (Cross 1988). Cells carrying this allele are able to proliferate even when the pheromone pathway is stimulated. The parent strain, however, also contains P_{GAL1}-GPA1-E364K, the hyperadaptive *GPA1* allele E364K, under the control of an attenuated *GAL1* promoter, *GAL1-EG28* (Stratton *et al.* 1996). Because Gpa1-E364Kp blocks pheromone-induced activity of the *FUS1* promoter (Stone and Reed 1990), cells are unable to grow on galactose-based medium containing pheromone and lacking leucine. The basis for the selection of Adp$^-$ mutants, then, is that mutations that interfere with the ability of Gpa1p to stimulate adaptation should allow *FUS1-LEU2* induction.

Approximately 2×10^7 cells were mutagenized on plates, and with the P_{GAL1}-*GPA1-E364K* construct induced, they were replica plated to medium containing pheromone and lacking leucine. To sort out the desired mutations from an unwanted background (*e.g.*, mutations that knock out the expression or function of P_{GAL1}-*GPA1-E364K*), colonies recovered in this selection were screened for a heightened response to pheromone with the expression of *GPA1-E364K* repressed. Mutations that blocked Gpa1-E364Kp–mediated adaptation and that conferred supersensitivity by themselves were considered likely to be in genes encoding its effector or downstream elements in its signaling pathway.

Colonies picked from the primary selection plates were cured of the *GAL1-CLN3-2* vector and then tested for their ability to grow at various concentrations of α factor in single-colony formation and halo assays under both P_{GAL1}-*GPA1-E364K*–expressing and –repressing conditions. Of the roughly 1000 mutants isolated in this selection that were able to induce *FUS1-LEU2* despite expression of *GPA1-E364K*, about one-quarter exhibited a phenotype that was dramatic enough to warrant further analysis. These 253 mutants fell into two classes. The 183 class I mutants showed an extreme sensitivity to pheromone when *GPA1-E364K* expression was turned off, as manifested by very large halos, but were uncompromised in their ability to adapt to pheromone treatment when the mutant *GPA1* allele was turned on, as evidenced by very turbid halos (see Figure 1). Many of these mutants showed an increased expression of *FUS1-LEU2* and displayed mating-specific morphological changes in the absence of pheromone, indicating an elevation in the basal pheromone pathway activity. Presumably, class I mutations augment the mating signal to such a degree that the Gpa1p-mediated adaptive signal is partially overridden, and the *FUS1-LEU2* construct is induced sufficiently to generate Leu$^+$ colonies. Characterization of these mutants will be described elsewhere. In contrast to the highly supersensitive/Adp$^+$ phenotype of class I mutants, the 70 class II mutants were slightly supersensitive and Adp$^-$ (Figure 1): They were clearly compromised in their ability to recover from pheromone treatment when *GPA1-E364K* was expressed (as evidenced by clear or lightly filled halos), and they showed a slightly greater than normal response when the hyperadaptive *GPA1* allele was repressed (as evidenced by large halos). Like the class I mutants, the class II mutants fell into two subgroups: those that were leucine prototrophs, even in the absence of pheromone (*i.e.*, they exhibited a high basal pathway activity), and those that required pheromone to induce the *FUS1-LEU2* construct.

To test the Adp$^-$ mutations for dominance, the class II mutants were crossed to a specialized strain designed to allow recovery of *MAT***a**/*mat*Δ diploids (see materials and methods). The dominance relationships of mutations affecting the yeast pheromone response must be tested in diploids expressing only *MAT***a** information because *MAT***a**/*MAT*α strains do not express the mating response pathway and are therefore sterile. For those mutations that conferred a constitutive Leu$^+$ phenotype, dominance was assessed by simply scoring the diploids for leucine prototrophy. Additionally, all *MAT***a**/*mat*Δ diploids carrying Adp$^-$ mutations were subjected to halo tests on P_{GAL1}-*GPA1-E364K*–inducing medium. Failure of a given diploid to form colonies within the halo zone was taken as an indication that the mutation in question was dominant. Because we expected the Adp$^-$ phenotypes to result from loss-of-function mutations, it was surprising to find that of the 49 class II mutants analyzed in this study, 37 were dominant and only 12 were recessive.

Dominant missense mutations in *STE4* block Gpa1p-mediated adaptation: The pheromone-responsive G_β of yeast, Ste4p, is rapidly phosphorylated when cells are treated with α factor, and this modification is thought to be an adaptive mechanism (Cole and Reed 1991). Deletion of the putative phosphorylation domain of Ste4p, residues 310–346, confers supersensitivity (Cole and Reed 1991) and blocks Gpa1p-mediated adaptation (D. E. Stone and H. F. Stratton, unpublished results).

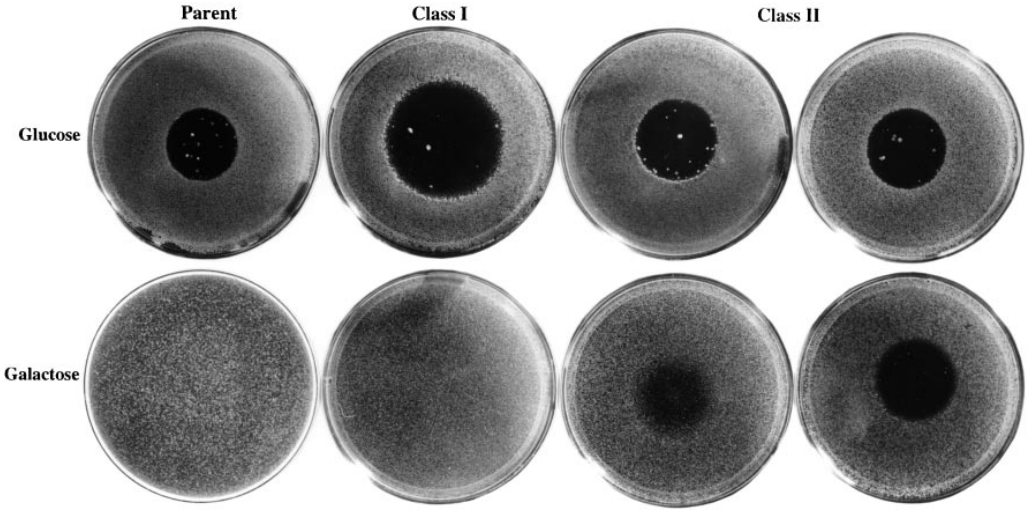

Figure 1.—Halo tests showing representative class I and II mutants. The parent strain and all the mutants contain the P_{GAL1}-*GPA1-E364K* fusion that is repressed by glucose and induced by galactose. Cells were grown in rich glucose medium (top row) or rich galactose medium (bottom row), and halo tests were performed on the corresponding medium using 4 μg of α factor. Class I mutants are supersensitive/adaptive$^+$. Class II mutants are supersensitive/Adp$^-$.

In other words, the *STE4*$^{\Delta 310\text{-}346}$ allele is epistatic to *GPA1-E364K*. Deletion of this domain also prevents certain signaling-defective forms of Ste4p from promoting adaptation (Grishin *et al.* 1994). The recovery of such a high proportion of dominant Adp$^-$ mutants in our screen led us to speculate that novel alleles of *STE4* were represented in the collection. In particular, we expected to find lesions in the 310–346 region of Ste4p. Therefore, we asked whether dominant Adp$^-$ mutations could be separated from *STE4* in linkage analysis. Ten strains carrying such mutations, each of which conferred a constitutively active *FUS1-LEU2* phenotype that resulted in leucine prototrophy and which segregated as single loci, were crossed to a congenic *MAT*α tester strain. Like the mutant strains, the tester strain contained the *FUS1-LEU2* reporter construct. In addition, the *STE4* locus of this strain was marked with the *LEU2* gene. Diploids resulting from crosses between the *MAT***a** *FUS1-LEU2 leu2*$^-$ Adp$^-$ mutants and the *MAT*α *FUS1-LEU2 leu2*$^-$*ste4*Δ*::LEU2* tester were sporulated and dissected. A meiotic segregant is expected to be prototrophic for leucine if it inherits either the *ste4*Δ*::LEU2* construct or the Adp$^-$ mutation (which activates *FUS1-LEU2*). If the Adp$^-$ mutation is in *STE4*, then all segregants are expected to be Leu$^+$ because the *ste4*Δ*::LEU2* construct will always segregate away from the *STE4* Adp$^-$ allele. Of the 10 mutants analyzed in this manner, eight yielded 100% Leu$^+$ segregants in 12 tetrads. These results strongly suggest that mutations in *STE4* are responsible for the dominant Adp$^-$ phenotype in the majority of these mutant strains.

To recover the *STE4* alleles from the strains showing tight linkage between the adaptive mutation and the *STE4* locus, the gap repair method described by Orr-Weaver *et al.* (1983) and Rothstein (1991) was used. The mutant strains were transformed with a gapped *STE4* plasmid, and plasmids repaired *in vivo* (presumably by recombination with the mutant *STE4* allele) were extracted. Rescued plasmids that could confer the original dominant Adp$^-$ phenotype upon transformation of the unmutagenized parent strain were sequenced across the *STE4* coding region. The results of this analysis are shown in Figure 2 and Table 1. In each case, the rescued *STE4* allele differed from the published *STE4* sequence (Whiteway *et al.* 1989) in two positions. Nucleotide 709 was invariably found to be C instead of T, which is predicted to result in the substitution of serine for leucine at residue 236. This apparent polymorphism was confirmed by sequencing the wild-type allele of *STE4* from strain 15Dau. Each rescued allele was also found to differ from the wild-type sequence at one additional site. The seven novel *STE4* mutations cluster in two regions: a C-terminal group includes substitutions in residues 405, 409, 410, and 411; an N-terminal group includes substitutions at residues 115 and 138. The *STE4-S410L* allele was recovered independently three times, suggesting that many of the *STE4* mutations generated in this screen have been identified.

$G_{\beta\gamma}$ subunits containing the dominant Adp$^-$ forms of Ste4p can be sequestered by Gpa1p: All seven of the Adp$^-$ strains listed in Table 1 are leucine prototrophs, presumably because the *STE4* Adp$^-$ alleles that they carry raise the activity of the basal mating signal enough to induce the expression of *FUS1-LEU2*. None of these strains, however, exhibit the changes in morphology and growth rate that are expected to result from a high

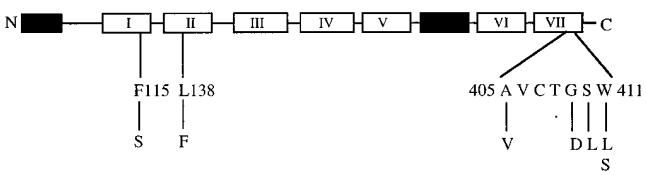

Figure 2.—Positions of the mutations and the resulting substitutions in the *STE4* Adp$^-$ alleles. The open boxes represent the WD40 repeat units found in all G_β subunits. The shaded boxes represent the domains unique to Ste4p.

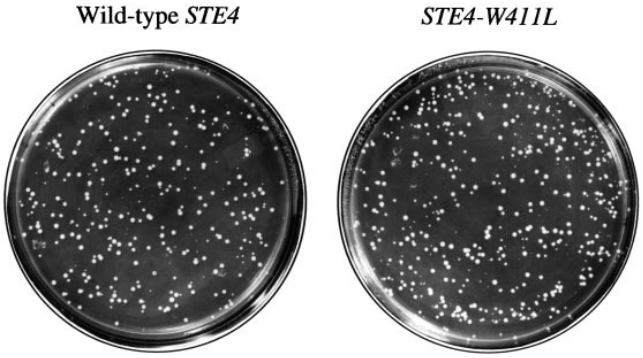

Figure 3.—Plating efficiency and colony size of the *STE4-W410L* Adp$^-$ mutant in comparison to wild-type cells. Centromeric plasmids containing either the wild-type or a mutant allele of *STE4* were transformed into strain 15Dau *bar1*Δ *ste4*Δ*::LEU2*. The resulting transformants were spread at an equal density on plates and incubated at 30° for 3 days. The colony sizes and densities were indistinguishable for all the mutants and the wild-type allele of *STE4*, except for *STE4-F115S* cells, which formed noticeably smaller colonies.

basal mating signal. Because even a slight increase in the basal signal could create a selective pressure for sterile mutations or result in physiological adaptation, such mutant phenotypes could be lost over time. A derivative of wild-type strain 15Dau in which the native *STE4* allele had been deleted was therefore transformed with the gap-repaired yeast centromeric vectors containing the *STE4* Adp$^-$ alleles. With the exception of the *STE4-F115S* cells, each of the newly created mutant strains grew normally (Table 1), forming visible colonies at a rate indistinguishable from 15Dau *ste4*Δ cells transformed with a plasmid-borne copy of wild-type *STE4* (Figure 3). Moreover, examination of the mutant cells under the light microscope revealed no sign of projection formation (shmooing), the morphological change particular to cells responding to pheromone (data not shown). Assuming that Ste4p reaches its normal steady-state level and is localized within the time it takes the transformed cells to go through one or two generations (2–4 hr), the growth rate of the transformed colonies provides a sensitive means to assess the ability of Gpa1p to bind the mutant forms of G_β. A defect in α–$\beta\gamma$ binding caused by a mutation in *STE4* should lead to activation of the mating signal and, hence, projection formation and inhibition of growth, as has been observed in cells expressing *STE4*^{Hpl} alleles (Blinder *et al.* 1989; Whiteway *et al.* 1994). Although the original mutant strains may have undergone genetic changes that normalized the basal signal during their isolation, introduction of the *STE4* Adp$^-$ alleles into a clean genetic background and immediate assessment of the transformed cells eliminates this variable.

Cells expressing *STE4* Adp$^-$ alleles grow normally in the absence of pheromone, but their growth is arrested by doses of α factor that wild-type cells are able to overcome (Table 1 and Figure 4). Is this supersensitive phenotype caused by a defect in α–$\beta\gamma$ affinity? As a second means of assessing the ability of Gpa1p to bind the mutant forms of G_β, halo tests were performed on *STE4* Adp$^-$ cells expressing either E364K or G322E, two mutant alleles of *GPA1*. Although *GPA1-E364K* and *GPA1-G322E* both confer resistance to pheromone, they act by different mechanisms (Stratton *et al.* 1996). Whereas Gpa1-E364Kp stimulates adaptation (recovery from pheromone treatment), Gpa1-G322Ep confers insensitivity (an inability to respond to pheromone). Based on the biochemical characterization of an analogous mutant form of $G_{\alpha s}$ (Lee *et al.* 1992), as well as on genetic (Stratton *et al.* 1996) and biochemical (M. Cismowski and D. Stone, unpublished results) evidence, Gpa1-G322Ep is thought to confer resistance to pheromone by sequestering $G_{\beta\gamma}$. Thus, if Gpa1p can bind $G_{\beta\gamma}$ in spite of the mutations in *STE4*, then *GPA1-G322E* should

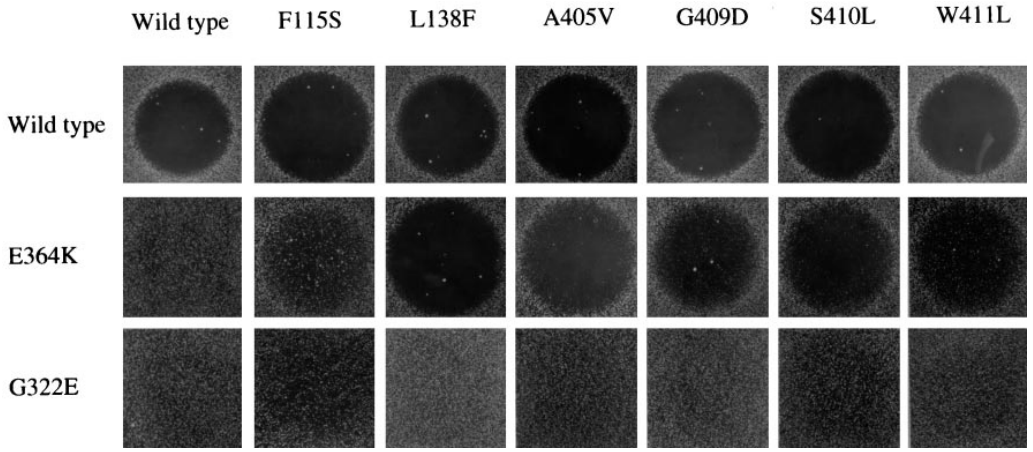

Figure 4.—Epistasis analysis. Halo tests showing the ability of *GPA1-E364K* and *GPA1-G322E* to confer pheromone resistance in the various *STE4* Adp$^-$ mutant backgrounds. Cells were grown in synthetic medium lacking uracil to select for the *GPA1* vectors, and halo tests were performed on the corresponding medium using 4 μg of α factor. The area around the point source of pheromone was photographed after 2 days of incubation at 30°. All magnifications are equivalent.

be epistatic to the *STE4* Adp$^-$ alleles. As shown in Figure 4, cells expressing Gpa1-G322Ep and wild-type Ste4p were almost completely resistant to α factor. With the exception of the cells transformed with the *STE4-F115S* allele, which formed a very turbid halo, the strains expressing *GPA1-G322E* and the *STE4* Adp$^-$ alleles were similarly unresponsive. In contrast, the hyperadaptive phenotype conferred by *GPA1-E364K* in cells expressing wild-type *STE4*, as evidenced by turbid halos, was much less apparent in cells expressing the *STE4* Adp$^-$ alleles.

Effects of the dominant Adp$^-$ *STE4* mutations on mating-specific transcription: In addition to its effects on growth and cellular morphology, pheromone stimulates the transcription of genes that are required for modulation of the mating signal and for cell and nuclear fusion. In fact, measuring the expression of mating-specific genes is a more sensitive means to assess mating pathway activity than are the cellular responses to pheromone (Cross *et al.* 1988). Transcriptional assays are also more informative over a much shorter time period than are colony forming assays, such as halo tests. To determine how the *STE4* Adp$^-$ mutations affect the transcriptional activity of mating-specific genes, we transformed six of the seven original mutant strains with *FUS1-lacZ::ADE1*, a centromeric vector containing a transcriptional fusion between the *FUS1* promoter region and the lacZ coding sequence. Like the native *FUS1* gene, the expression level of the *FUS1-lacZ* reporter construct is proportional to the activity of the pheromone signaling pathway: its expression is dependent on an intact signaling pathway and is strongly induced by pheromone. The mutant strains and a wild-type control strain, each carrying the reporter vector and a centromeric plasmid containing *GPA1*, were grown to midlog phase and sampled for basal pathway activity. They were then treated with a submaximal dose of α factor for 4 hr, and samples were harvested for determination of β-galactosidase activity. As shown in Figure 5A, the basal activity

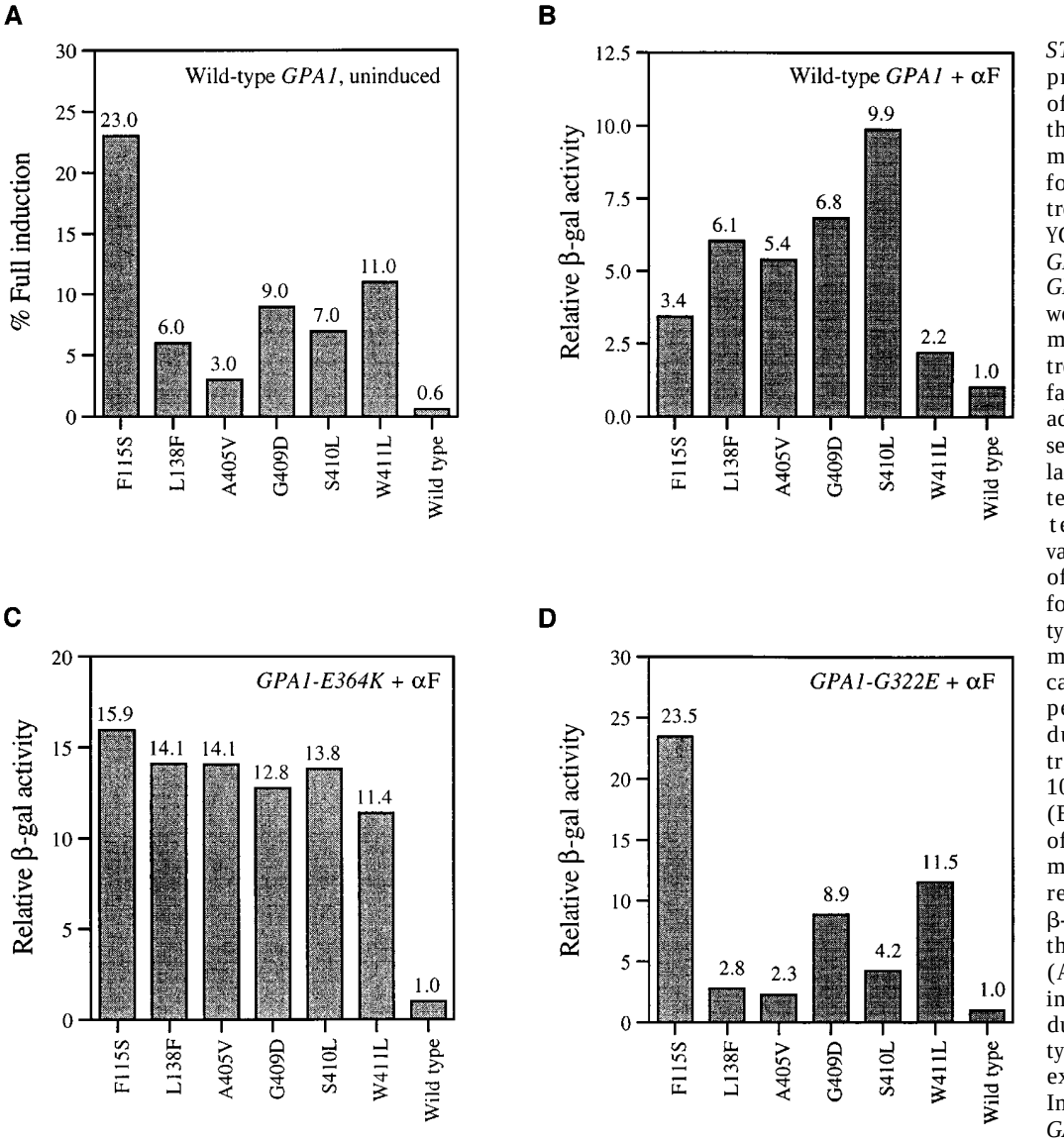

Figure 5.—Effects of the *STE4* Adp$^-$ alleles when expressed with various forms of Gpa1p on the activity of the *FUS1* promoter. The mutant strains were transformed with a *FUS1-lacZ* centromeric plasmid and either YCplac33/*GPA1*, YCplac33/*GPA1-E364K*, or YCplac33/*GPA1-G322E*. Transformants were grown to midlogarithmic phase and were either treated with 20 ng/ml of α factor for 4 hr or grown an additional 4 hr in the absence of pheromone. β-Galactosidase levels were determined as described in materials and methods. The values shown are the mean of duplicate determinations for each strain. The data are typical of numerous experiments. (A) The value indicated for each mutant is the percent of full *FUS1-lacZ* induction, as determined by treating wild-type cells with 100 ng/ml α factor for 4 hr. (B–D) The induced levels of β-galactosidase in the mutant cells are expressed relative to the induced β-galactosidase activity in the wild-type control cells. (A) Uninduced cells expressing wild-type *GPA1*. (B) Induced cells expressing wild-type *GPA1*. (C) Induced cells expressing *GPA1-E364K*. (D) Induced cells expressing *GAL1-G322E*.

of the mating signal was variously affected by the *STE4* Adp$^-$ mutations. The *STE4-F115S* allele caused the greatest increase in basal *FUS1-lacZ* activity (~23% of full induction), the L138F substitution and the three-most C-terminal mutations in *STE4* caused a moderate increase in the constitutive signal (6–11% of full induction), and the *STE4-A405V* cells showed the smallest increase in the steady-state lacZ expression (~3% of full induction). After treatment with a low concentration of α-factor, the mutant strains all displayed supersensitivity, producing two to 10 times more β-galactosidase than the wild-type control cells (Figure 5B). Induction of *FUS1-lacZ* was similar in all the strains after a saturating dose of α factor (data not shown). In comparing the mutant strains, no correlation between the degree of basal signaling and the degree of supersensitivity was apparent. Identical experiments performed with strains in which the *STE4* Adp$^-$ alleles had been introduced into a clean genetic background by transplacement of wild-type *STE4* produced similar results, although the basal activities of the mutant strains were not as highly induced (data not shown).

Because the Adp$^-$ mutants were originally selected as cells that could induce *FUS1-LEU2* in spite of *GPA1-E364K* expression, we assessed the ability of Gpa1-E364Kp to repress mating-specific transcription in the *STE4* Adp$^-$ backgrounds. The *STE4* Adp$^-$ mutant strains were transformed with *FUS1-lacZ::ADE1*, and a centromeric plasmid containing the *GPA1-E364K* coding region under the control of the *GPA1* promoter (YCplac33/*GPA1-E364K*). The resulting transformants were then grown to midlog phase, and β-galactosidase activity was measured before and 4 hr after treatment with a submaximal dose of α factor. As shown in Figure 5C, the adaptive function of Gpa1-E364Kp was severely compromised in all six of the *STE4* Adp$^-$ mutants tested: the induced β-galactosidase rose to levels 11.4- to 15.9-fold higher than in the wild-type control strain. As we observed in cells expressing the wild-type allele of *GPA1*, the induced *FUS1-lacZ* activities in the mutant strains expressing *GPA1-E364K* showed no correlation with the increases in basal *FUS1-lacZ* activity.

The superinduction of the *FUS1* promoter could be caused either by the inability of Gpa1p to sequester the mutant forms of $G_{\beta\gamma}$ after pheromone treatment or by the failure of a protein other than Gpa1p to downregulate the aberrant $G_{\beta\gamma}$ subunits. To distinguish these possibilities, the ability of the G322E mutant form of Gpa1p to inhibit *FUS1-lacZ* activity in the *STE4* Adp$^-$ strains was assessed. Gpa1-G322Ep negatively regulates the mating signal by sequestering $G_{\beta\gamma}$. Mutant cells transformed with both the *FUS1-lacZ* reporter vector and a centromeric plasmid containing the *GPA1-G322E* coding region under the control of the *GPA1* promoter (YCplac33/*GPA1-G322E*) were treated with α factor, and the induced β-galactosidase levels were measured, as described above. The results of this experiment, shown in Figure 5D, are striking. The induced β-galactosidase levels in the various mutants expressing Gpa1-G322Ep varied over a 10-fold range, just as the basal *FUS1-lacZ* activities did (Figure 5A). Moreover, a comparison of the mutants to one another revealed the same relationships that were observed when the basal activities were measured (Figure 5A). For example, the Adp$^-$ form of Ste4p that caused the highest basal *FUS1* activity (Ste4-F115Sp) was least affected by Gpa1-G322Ep expression, whereas the mutant G_β that caused the smallest increase in basal *FUS1* activity (Ste4-A405Vp) was most effectively inhibited by Gpa1-G322Ep.

Pheromone-induced phosphorylation of the dominant Adp$^-$ forms of Ste4p is normal: Because pheromone-induced phosphorylation of Ste4p is thought to be an adaptive mechanism that is dependent upon Gpa1p (Cole and Reed 1991), and because the *STE4* Adp$^-$ mutants block Gpa1p-mediated adaptation, it was of interest to determine whether the adaptive defects are caused by an inability to phosphorylate Ste4p. The effect of the Adp$^-$ mutations on Ste4p phosphorylation was assessed by monitoring the migration of Ste4p on denaturing polyacrylamide gels, taking advantage of the observation that pheromone-induced phosphorylation of Ste4p leads to a characteristic reduction in its electrophoretic mobility (Cole and Reed 1991). The results of an experiment in which wild-type and mutant cells were treated with a submaximal dose of pheromone for a period of 2 hr are shown in Figure 6. Proteins extracted from each culture were electrophoresed, blotted to nitrocellulose, and probed with an affinity-purified anti-Ste4p polyclonal antibody. Consistent with previously reported results, the phosphorylation state of Ste4p changed dramatically when wild-type cells were exposed to α factor. The bulk of the protein was chased from the fastest migrating (relatively unphosphorylated) spe-

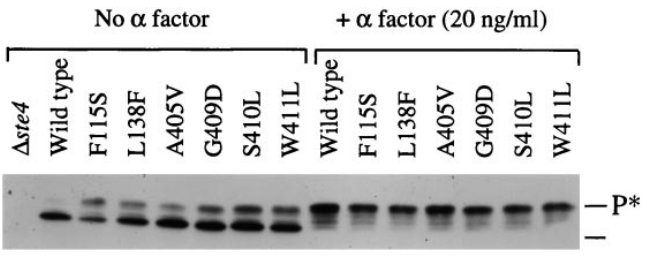

Figure 6.—Phosphorylation state of Ste4p in *STE4* Adp$^-$ mutant and wild-type cells. Midlogarithmic phase mutant and wild-type cells were grown in the absence of pheromone or treated with various doses of α-factor for 2 hr, as indicated. Crude lysates were prepared as described in materials and methods, and electrophoresed on denaturing polyacrylamide gels. Proteins were then blotted to polyvinyldifluoride membranes and probed with an affinity-purified antibody raised against Ste4p. The rate of migration of the Ste4p protein is a function of its phosphorylation state: the unphosphorylated form (dash) migrates fastest; the fully phosphorylated form (P*) migrates slowest.

cies of Ste4p in the untreated control to the slowest migrating (fully phosphorylated) species of Ste4p at 20 ng/ml α factor, half the dose that is required to block cell cycle progression under these culture conditions. Identical results were obtained when cells were challenged with 100 ng/ml of α factor (data not shown). Interestingly, all six of the *STE4* Adp$^-$ strains tested in this assay were fully responsive, exhibiting no defect in Ste4p phosphorylation. Therefore, the Adp$^-$ phenotypes cannot be attributed to a failure to modify the mutant forms of G_β. Before pheromone stimulation, however, the six *STE4* Adp$^-$ strains did show a detectable increase in the basal level of Ste4p phosphorylation. By comparing the intensity of the uppermost band to that of the lowermost band in lanes 1–7 of Figure 6, it is apparent that there is some variation in the mutant phenotypes: Ste4-F115Sp exhibited the greatest basal phosphorylation, whereas Ste4-A405Vp appeared most similar to wild type. The remaining mutants displayed an intermediate increase in the ratio of phosphorylated to unphosphorylated Ste4p. These data are consistent with the effects that the *STE4* Adp$^-$ alleles had on *FUS1-lacZ* activity (Figure 5).

Gpa1p does not stimulate phosphorylation of G_β: Based on the observation that Ste4p phosphorylation is dramatically impaired in a *gpa1*Δ strain (Cole and Reed 1991), it has been suggested that Gpa1p stimulates this modification of Ste4p, thereby promoting an adaptive mechanism. The identification of mutations in *STE4* that block Gpa1p-mediated adaptation, while having no effect on pheromone-induced phosphorylation of Ste4p, calls this hypothesis into question. To test this idea in a different way, wild-type cells were transformed with single-copy plasmids containing either *GPA1-E364K* or wild-type *GPA1*, and were treated with various concentrations of pheromone for a period of 2 hr. If Gpa1p downregulates the mating response by inducing Ste4p phosphorylation, a hyperadaptive allele of *GPA1* such as E364K would be expected to augment pheromone-induced phosphorylation of Ste4p. As shown in Figure 7, Gpa1-E364Kp did not stimulate Ste4p phosphorylation. In fact, close examination of Figure 7A reveals a

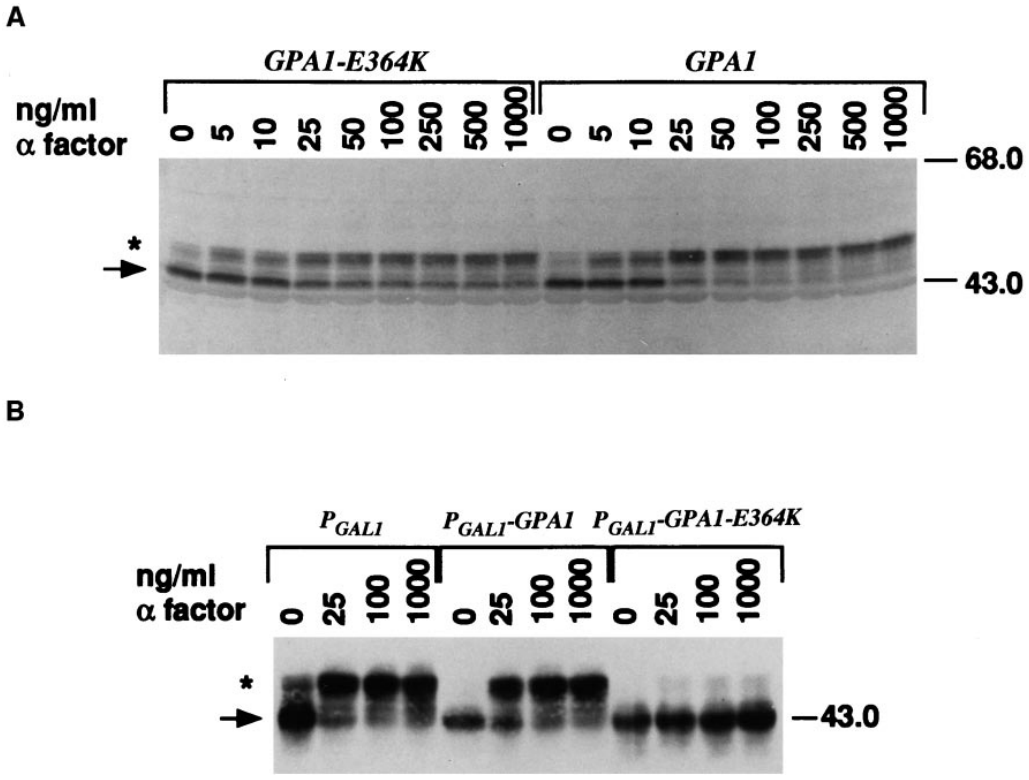

Figure 7.—Pheromone-induced phosphorylation of Ste4p in wild-type and cells expressing *GPA1-E364K*. Midlogarithmic phase cells were treated with the indicated doses of α factor for 2 hr. Immunoblots were prepared as described in materials and methods and probed with an affinity-purified antibody raised against Ste4p. The rate of migration of the Ste4p protein is a function of its phosphorylation state: the unphosphorylated form (arrow) migrates fastest; the fully phosphorylated form (star) migrates slowest. Molecular weights are in kilodaltons. (A) Wild-type cells were transformed with either an *GPA1-E364K* centromeric plasmid (YCplac111/*GPA1-E364K*) or an identical plasmid containing wild-type *GPA1* (YCplac111/*GPA1*). These strains express approximately the wild-type level of Gpa1p. (B) Wild-type cells transformed either with the *GAL1* centromeric expression vector YCpG2 or with YCpG2 carrying *GAL1-E364K* or *GAL1-GPA1*. The latter two strains overexpress Gpa1p by a factor of at least 10, as determined by scanning immunoblots (data not shown) probed with strip-purified antisera raised against Gpa1p (Stone *et al.* 1991).

slight inhibitory effect on this phenomenon (compare the ratio of the highest and lowest bands in the wild-type and *GPA1-E364K* cells, especially at doses >50 ng/ml). Although the magnitude of this effect is small, the result is significant. A similar effect was found in cells expressing wild-type levels of Gpa1-E364Kp when Ste4p phosphorylation was examined as a function of time (data not shown). Moreover, the phosphorylation of Ste4p was almost completely blocked when the *GAL1* promoter was used to drive overexpression of *GPA1-E364K* (Figure 7B).

Since the experimental cells used in these assays were constitutively expressing *GPA1-E364K*, we considered the possibility that the Gpa1p-mediated adaptive pathway might itself be downregulated as a consequence of chronic activation, thus minimizing Gpa1-E364Kp–induced phosphorylation of Ste4p. To prevent such long-term physiological changes, the P_{GAL1}-*GPA1* cells and P_{GAL1}-*GPA1-E364K* cells were cultured under noninducing conditions, and the *GAL1* promoter was induced concomitantly with the addition of pheromone. Using this protocol, dose–response curves and time courses were generated, but in no case was *GPA1-E364K* expression correlated with increased phosphorylation of Ste4p (data not shown).

DISCUSSION

The realization that the βγ as well as the α subunits of heterotrimeric G proteins are active signaling elements in numerous systems (Clapham and Neer 1993; Iniguez-Lluhi *et al.* 1993) raises the question as to how the independent branches of G protein–mediated signaling pathways are functionally related, and how they are regulated. *A priori*, one can imagine systems in which G_α and $G_{\beta\gamma}$ regulate different effectors and systems in which they act on the same effector. In principle, the effects of G_α and $G_{\beta\gamma}$ stimulation could be additive, synergistic, or antagonistic. In fact, examples of each type are known (Clapham and Neer 1993).

The yeast mating response, which is driven by the βγ subunit of a G protein, provides an example of antagonistic regulation. We have shown that the pheromone-inducible G_α protein Gpa1p stimulates an adaptive signal that downregulates the $G_{\beta\gamma}$-induced mating signal independently of $G_{\beta\gamma}$ sequestration (Stratton *et al.* 1996). To identify elements downstream of Gpa1p in this pathway, we conducted a genetic screen for adaptive defects in a strain expressing a hyperadaptive allele of *GPA1*. Both recessive and dominant Adp$^-$ mutations were recovered. Eight out of the 10 dominant mutations tested showed tight linkage to *STE4*. Sequence analysis of the *STE4* locus in these mutant strains revealed seven novel *STE4* alleles—F115S, L138F, A405V, G409D, S410L, W411L, and W411S—each of which were shown to disrupt proper regulation of the pheromone response. The genetic characterization of these mutant forms of G_β led to two conclusions: (1) $G_{\beta\gamma}$ is a target of G_α-mediated adaptation and (2) the adaptive mechanism or mechanisms impaired by the lesions in *STE4* do not involve G_β phosphorylation.

$G_{\beta\gamma}$ is a target of Gpa1p-mediated adaptation: The mutant alleles of *STE4* isolated in this work confer a defect in regulation of the mating signal, especially in recovery from exposure to pheromone. It has been suggested that Ste4p negatively regulates the pheromone response in addition to stimulating it (Grishin *et al.* 1994). If Ste4p works in concert with Gpa1p to stimulate adaptation, mutations resulting in the loss of this function should be recessive. The discovery of mutations in *STE4* that disrupt Gpa1p-mediated adaptation and that are dominant suggests that Ste4p is a target of, rather than a cofactor in, the G_α-induced desensitization mechanism. The lesions in question presumably render G_β refractory to this adaptive mechanism.

Could the Adp$^-$ mutations in *STE4* simply disrupt α–βγ binding? Two pieces of evidence argue against this possibility. First, the mutant forms of Ste4p have relatively large effects on the induced signal in comparison to their effects on the basal signal. With the exception of the F115S mutation, the alterations in *STE4* had virtually no significant impact on the growth and morphology of cells cultured in the absence of pheromone, and only small effects on the steady-state levels of mating-specific transcription and Ste4p phosphorylation (Table 1 and Figures 3, 5, and 6). One *STE4* Adp$^-$ strain, *STE4-A405V*, was almost indistinguishable from wild type when grown in the absence of pheromone. After stimulation with pheromone, however, the effects of the *STE4* Adp$^-$ alleles were dramatic: cells coexpressing a *STE4* Adp$^-$ allele with wild-type Gpa1p formed larger than normal halos (Table 1 and Figure 4, top row); those expressing a *STE4* Adp$^-$ allele with the hyperadaptive allele of *GPA1*, E364K, showed significantly less colony formation within the halos than cells expressing *GPA1-E364K* and wild-type *STE4* (Figure 4, middle row). Thus, it appears that inactivation of the aberrant $G_{\beta\gamma}$ subunits is normal or nearly normal in the absence of pheromone, but is defective after pheromone treatment.

The results of the experiments designed to measure the effects of the *STE4* Adp$^-$ alleles on mating-specific transcription, which is more sensitive to pheromone stimulation than are the cellular responses, also suggest that the mutations primarily affect downregulation of the induced mating signal rather than basal pathway activity. In examining the transcriptional data, it is helpful to rank the mutants according to their relative β-galactosidase levels. The effects of the various *STE4* mutations on basal *FUS1-lacZ* transcription are widely variable: the *STE4-F115S* allele induces the highest constitutive activity, *STE4-A405V* has the least effect on transcription, and the other alleles are intermediate in this regard (Figure 5A). After treatment with a low dose of pheromone, the mutant strains expressing wild-type

Gpa1p exhibited between 2- and 10-fold supersensitivity (Figure 5B); those expressing *GPA1-E364K* all hyperinduced *FUS1-lacZ* to a similar level, 11–16-fold higher than the control (Figure 5C). Moreover, the rank order of the induced and basal *FUS1-lacZ* activities did not correlate in cells expressing either wild-type Gpa1p or Gpa1-E364Kp. In the wild-type *GPA1* background, for example, the allele that showed the greatest supersensitivity, *STE4-S410L*, exhibited one of the lowest basal activities. Similarly, the mutants that exhibited the highest basal activities were most effectively downregulated by Gpa1-E364Kp, whereas *FUS1-lacZ* was not downregulated as well by Gpa1-E364Kp in those mutants with the lowest basal activities. The lack of correspondence between the effect of a given *STE4* allele on basal and induced mating-specific transcription is significant. If the regulatory defect were simply caused by poor α–$\beta\gamma$ binding, then the mutations that most dramatically affect $G_{\beta\gamma}$ sequestration in the absence of pheromone might be expected to have the most adverse effect on recovery.

The second argument against the idea that the *STE4* Adp$^-$ mutations merely cause dissociation of the G protein subunits relies on experiments with G322E, a mutant form of Gpa1p that confers insensitivity to pheromone by sequestering $G_{\beta\gamma}$ (Stratton *et al.* 1996; M. Cismowski and D. Stone, unpublished results). As discussed above, the hyperadaptive form of Gpa1p, E364K, cannot fully stimulate recovery from pheromone treatment in cells expressing any of the *STE4* Adp$^-$ alleles (Figures 4, middle row, and 5). The *STE4* Adp$^-$ mutations are epistatic to *GPA1-E364K*. In contrast, the ability of Gpa1-G322Ep to sequester $G_{\beta\gamma}$ and block the mating response, as assayed in halo tests, is unaffected in all but one of the mutant strains (Figure 4, bottom row). The *STE4-F115S* mutant cells were the exception, forming detectable halos in spite of Gpa1-G322Ep expression. The difference in the effects of the *STE4* Adp$^-$ alleles on cells expressing these two functionally dissimilar forms of Gpa1p is consistent with the idea that the Adp$^-$ mutations affect the mating signal primarily through a defect in Gpa1p-mediated adaptation rather than by disrupting the sequestration of $G_{\beta\gamma}$ by G_α. The transcriptional and Ste4p phosphorylation assays, however, demonstrate that the mutant forms of G_β do have some impact on basal signaling (Figures 5 and 6). The levels of *FUS1-lacZ* activity and Ste4p phosphorylation are elevated to a variable degree, depending on which allele is tested. Presumably, the small increases in constitutive *FUS1-lacZ* activity result from the release of $G_{\beta\gamma}$ from G_α. Consistent with this inference, Gpa1-G322Ep suppressed the various forms of G_β in an allele-specific manner. When the effect of coexpressing *GPA1-G322E* and the *STE4* Adp$^-$ alleles in cells treated with pheromone was examined at the transcriptional level, a striking similarity to the basal signaling activities of the *STE4* Adp$^-$ mutants expressing wild-type Gpa1p was seen (Figure 5, A and C). The *STE4* Adp$^-$ mutations that manifested the highest constitutive *FUS1-lacZ* activity, presumably those that are most disruptive to α–$\beta\gamma$ binding, were also least well suppressed by Gpa1-G322Ep in cells exposed to pheromone. In fact, the bar graphs representing these two data sets are almost superimposable. This correlation between basal *FUS1* activity in wild-type cells and induced *FUS1* activity in cells expressing Gpa1-G322Ep supports the idea that these measurements reflect α–$\beta\gamma$ affinity. Thus, the A405V form of Ste4p is the least disruptive, and the F115S form of Ste4p is most disruptive to α–$\beta\gamma$ binding. Note that although *STE4-A405V* has almost no impact on basal signaling, it confers as severe a defect in recovery from pheromone treatment as do any of the other alleles.

Taken together, the data discussed in this section indicate that one target of Gpa1p-mediated adaptation is $G_{\beta\gamma}$. The observed defect in downregulation conferred by the *STE4* Adp$^-$ alleles can be explained in two ways. Gpa1p might stimulate the binding of an unknown regulator to $G_{\beta\gamma}$, and the Adp$^-$ mutations might disrupt this interaction. Candidates for this regulator include Akr1 (Kao *et al.* 1996; Pryciak and Hartwell 1996), Syg1 (Spain *et al.* 1995), Cdc24 (Simon *et al.* 1995; Zhao *et al.* 1995), and Ste5 (Whiteway *et al.* 1995)—proteins that are all thought to interact with Ste4p *in vivo*. Alternatively, the Adp$^-$ forms of $G_{\beta\gamma}$ may simply be refractory to sequestration by Gpa1p after pheromone treatment, but more easily bound by Gpa1p during vegetative growth. Although our data are inconsistent with the idea that the *STE4* Adp$^-$ mutations merely cause the release of $G_{\beta\gamma}$ from Gpa1p, we cannot eliminate the possibility that they differentially affect the ability of Gpa1p to bind $G_{\beta\gamma}$ in vegetative and pheromone-treated cells. Slight defects in α–$\beta\gamma$ affinity could also be overcome by the induction of downstream adaptive mechanisms in dividing cells. In other words, our failure to observe projection formation (shmooing) and poor growth (Table 1 and Figure 3) in cells newly transformed with the various *STE4* Adp$^-$ alleles could conceivably be caused by a rapid change in cellular physiology.

Ste4p phosphorylation and Gpa1p-mediated adaptation: Like metazoan G_β subunits, Ste4p is made up of a repeating amino acid sequence motif of $\sim$40 residues. In addition to the seven repeat motifs found in metazoan G_β subunits, however, Ste4p contains two unique insertions, one at the amino terminus and another between repeat motifs five and six. When cells are exposed to pheromone, Ste4p is rapidly phosphorylated within the internal domain, residues 310–346 (Cole and Reed 1991; and E Li and D. Stone, unpublished results). Because this domain has been implicated in adaptation, we asked whether the *STE4* Adp$^-$ mutations affect the phosphorylation state of Ste4p. *A priori*, the Adp$^-$ phenotypes could be caused by an inability to phosphorylate Ste4p. As shown in Figure 6, this is clearly not the case.

After treatment with a submaximal dose of pheromone, the mutant forms of Ste4p were all fully phosphorylated. Our data are also inconsistent with the idea that Gpa1p stimulates Ste4p phosphorylation. Rather than augmenting phosphorylation of G_β, a hyperadaptive form of Gpa1p actually inhibits it (Figure 7). Thus, although these data are strictly correlative, our failure to observe a correspondence between adaptation and Ste4p phosphorylation indicates a need to reexamine the role of G_β modification in pheromone signaling.

Location of the Adp$^-$ mutations in the three-dimensional structure of G_β: The crystal structures of the $G_{\beta\gamma}$ dimer from mammalian retinal cells (transducin $\beta\gamma$) in its free form (Sondek *et al.* 1996), complexed with a chimeric form of α (Lambright *et al.* 1996), and complexed with retinal phosducin (Gaudet *et al.* 1996) have recently been solved. Because most of the contacts between α and β involve residues that are conserved in both proteins, the interactions observed in the α–$\beta\gamma$ crystal are likely to occur in other members of the heterotrimeric G protein family, including Gpa1p and Ste4p (Lambright *et al.* 1996). Structural information about the Ste4p residues implicated in adaptation is summarized in Table 2, and the locations of the corresponding residues in the transducin $\beta\gamma$ crystal are shown in Figure 8.

The transducin $\beta\gamma$ dimer is primarily a seven-bladed β-propeller. Each of the blades is a β sheet made of four antiparallel strands. The N-terminus of G_β forms an α helix that interacts with the first helix of the G_γ subunit, and the second helix and extended portions of G_γ partially encircle the β propeller. Interaction between G_α and $G_{\beta\gamma}$ occurs at two distinct interfaces. Residues in the loops and turns at the top of the β propeller domain of G_β (blades 2–5, and 7) interact with residues in or adjacent to the switch I and switch II region of G_α. This is called the switch interface. The second α–$\beta\gamma$ interface is formed by interaction between the N-terminal helix of G_α and the side of the first blade of the β propeller. This is called the N-terminal interface. The surface area of the N-terminal interface is about half that of the switch interface.

Because the structures of the free and α-bound forms of transducin $\beta\gamma$ are not significantly different, it is unlikely that the signaling activity of $G_{\beta\gamma}$ depends on a change in its conformation. Rather, key contact sites for $G_{\beta\gamma}$ effectors and regulators may be unmasked when the G protein subunits dissociate. By analogy to the mammalian α–$\beta\gamma$ crystal structure, three of the Ste4p residues identified in this study are located in the regions of α–$\beta\gamma$ interaction and are predicted to lie on the exposed surface of the free Ste4p-Ste18p dimer. Residues L138 (in blade 2) and W411 (in blade 7) are predicted to contact the switch region of Gpa1p; residue F115 (in blade 1) is predicted to contact the N-terminal helix of Gpa1p. In addition to interacting with Gpa1p, all three of these residues are readily accessible to effector and regulatory molecules. This raises the possibility that the Adp$^-$ forms of Ste4p prevent proper downregulation of the mating signal by hyperstimulating the mating effector. It is not necessary, however, to invoke gain-of-function mutations to explain the data. It is more plausible that F115S, L138F, W411L, and W411S are

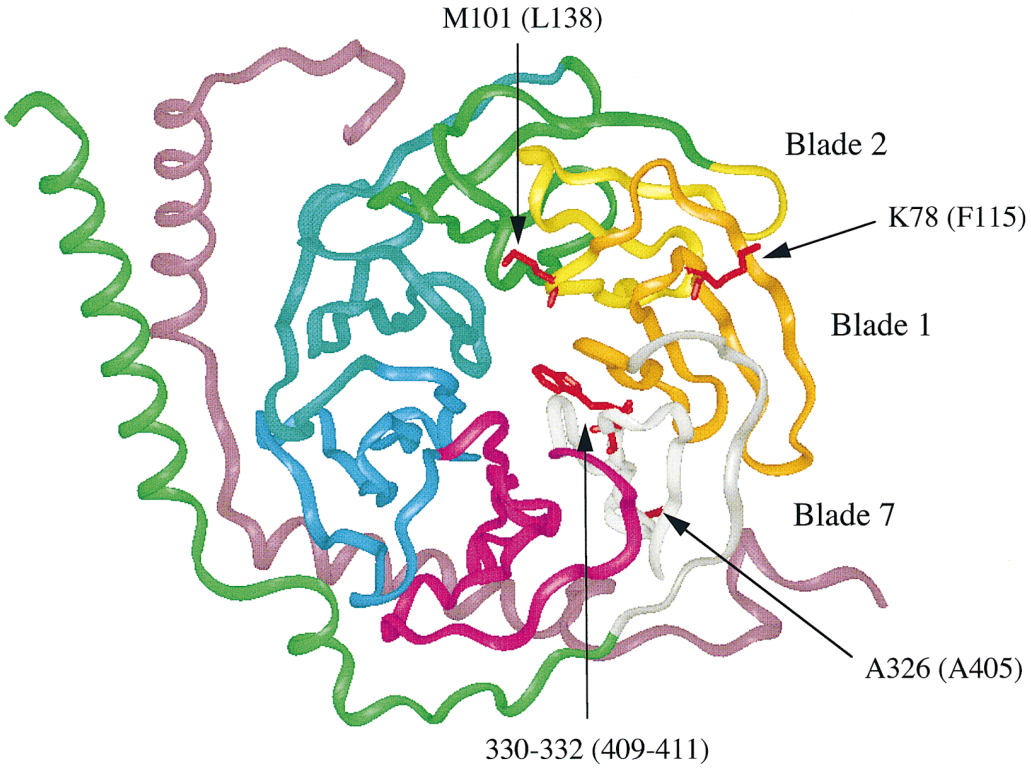

Figure 8.—Ribbon diagram of the transducin $\beta\gamma$ crystal structure. The N-terminal helix of transducin β and the blades of the propeller are distinguished by color. Transducin gamma is shown in purple. The transducin β residues that correspond to the substituted residues in the Adp$^-$ forms of Ste4p are shown in red and are labeled. The analogous residues of Ste4p are indicated in parentheses. The label 330-332 refers to G330, S331, and W332 of transducin β; 409-411 refers to G409, S410, and W411 of Ste4p.

TABLE 2

Inferences about the structure of the Adp$^-$ forms of Ste4p based on analogy to mammalian G proteins

Ste4p residue	Analogous position in transducin βγ crystal[a]	Adp$^-$ allele/type of substitution	Analogous residue in T_β	Interacting residues in T_α[c]	Putative interacting residues in Gpa1p	Type of interaction with α[c]	Interacting residues in phosducin[d]	Type of interaction with phosducin[d]
F115	Loop between second and third strand of blade 1	F115S/ nonconservative[b]	K78	L19 D22	L31 E34	van der Waals, ionic	—	—
L138	Beginning of first strand, blade 2	L138F/ conservative[b]	M101	H209	H232	van der Waals	I26	van der Waals
A405	End of loop between first and second strand, blade 7	A405V/ conservative	A326	—	—	—	—	—
G409	End of second strand, blade 7	G409D/ conservative	G330	—	—	—	—	—
S410	Loop between second and third strands, blade 7	S410L/ nonconservative	S331	—	—	—	—	—
W411	Loop between second and third strands, blade 7	W411L, W411S/ conservative	W332	H209	H232	van der Waals	M101 H102 L105	van der Walls

[a] Sondek *et al.* (1996).
[b] Determined according to Schwartz and Dayhoff (1979); a substitution is deemed conservative if the Dayhoff value is ≥0.4.
[c] Lambright *et al.* (1996).
[d] Gaudet *et al.* (1996).

loss-of-function mutations that prevent downregulation of $G_{\beta\gamma}$ by Gpa1p or by an unknown negative regulator. A precedent for such a molecule is phosducin, which downregulates $G_{\beta\gamma}$ moieties in a variety of metazoan systems. The recently solved crystal structure of the transducin βγ-retinal phosducin complex (Gaudet *et al.* 1996) reveals direct contacts between the N-terminal domain of phosducin (helices 1 and 3) and the residues of transducin G_β that are analogous to residues L138 and W411 of Ste4p. The structure of the transducin βγ–phosducin complex also suggests that phosducin induces a conformational shift in $G_{\beta\gamma}$. The positions of three loops at the top of blades 6 and 7 of the β propeller are changed upon $G_{\beta\gamma}$–phosducin binding. Interestingly, the most C-terminal of these loops corresponds to residues 408–417 of Ste4p. This suggests a mechanism by which the A405V, G409D, and S410L substitutions in Ste4p might prevent proper downregulation of the mating signal. Although the analogous residues of transducin G_β contact neither G_α or phosducin directly, substitutions at these positions might affect a local change in the conformation of the β propeller such that the binding of a negative regulator is inhibited.

In conclusion, although it is possible that the *STE4* Adp^- mutations preferentially disrupt sequestration of $G_{\beta\gamma}$ by G_α after pheromone treatment, we do not favor this idea. We propose that the pheromone-responsive yeast G_α protein Gpa1p stimulates an unknown molecule to bind and downregulate its βγ (Ste4p-Ste18p). The interaction between this putative downregulator and the Ste4p-Ste18p dimer is adversely affected by changes in Ste4p residues that are involved in direct contact (F115, L138, and W411) and by C-terminal mutations that impair an essential conformational shift (A405, G409, and S410). The F115S substitution most likely affects α–βγ binding as well as downregulation of $G_{\beta\gamma}$ by the unknown regulator.

The authors would like to thank Heidi Hamm for helpful discussions and for creating Figure 8; Fred Cross, Gary Cole, Phillip Nagley, and Hay-Oak Park for plasmids; and Mary Cismowski and Steve Reed for helpful discussions and for critical reading of the manuscript. This work was supported by an American Cancer Society Research grant (VM-92A) to D.E.S.

LITERATURE CITED

Ausubel, F. M., R. Brent, R. E. Kingston, D. D. Moore, J. G. Seidman *et al.*, 1994 *Current Protocols in Molecular Biology.* John Wiley & Sons, New York.

Blinder, D., S. Bouvier and D. D. Jenness, 1989 Constitutive mutants in the yeast pheromone response: ordered function of the gene products. Cell **56:** 479–486.

Clapham, D. E., and E. J. Neer, 1993 New roles for G-protein βγ-dimers in transmembrane signalling. Nature **365:** 403–406.

Cole, G. M., and S. I. Reed, 1991 Pheromone-induced phosphorylation of a G protein β subunit in *S. cerevisiae* is associated with an adaptive response to mating pheromone. Cell **64:** 703–716.

Cole, G. M., D. E. Stone and S. I. Reed, 1990 Stoichiometry of G protein subunits affects the *Saccharomyces cerevisiae* mating pheromone signal transduction pathway. Mol. Cell. Biol. **10:** 510–517.

Crespo, P., T. G. Cachero, N. Xu and J. S. Gutkind, 1995 Dual effect of β-adrenergic receptors on mitogen-activated protein kinase. Evidence for a βγ-dependent activation and a G_αs-cAMP-mediated inhibition. J. Biol. Chem. **270:** 25259–25265.

Cross, F., 1988 *DAF1*, a mutant gene affecting size control, pheromone arrest, and cell cycle kinetics of *Saccharomyces cerevisiae*. Mol. Cell Biol. **8:** 4675–4684.

Cross, F., L. H. Hartwell, C. Jackson and J. B. Konopka, 1988 Conjugation in *Saccharomyces cerevisiae.* Annu. Rev. Cell. Biol. **4:** 429–457.

Doi, K., A. Gartner, G. Ammerer, B. Errede, H. Shinkawa *et al.*, 1994 MSG5, a novel protein phosphatase promotes adaptation to pheromone response in *S. cerevisiae*. EMBO J. **13:** 61–70.

Gaudet, R., A. Bohm and P. Sigler, 1996 Crystal structure at 2.4 Å resolution of the complex of transducin βγ and its regulator, phosducin. Cell **87:** 577–588.

Gietz, R. D., and A. Sugino, 1988 New yeast—*Escherichia coli* shuttle vectors constructed with in vitro mutagenized yeast genes lacking six-base pair restriction sites. Gene **74:** 527–534.

Grishin, A. V., J. L. Weiner and K. J. Blumer, 1994 Control of adaptation to mating pheromone by G protein β subunits of *Saccharomyces cerevisiae*. Genetics **138:** 1081–1092.

Harlow, E., and D. Lane, 1988 *Antibodies: A Laboratory Manual.* Cold Spring Harbor Laboratory, Cold Spring Harbor Press, NY.

Iniguez-Lluhi, J., C. Kleuss and A. G. Gilman, 1993 The importance of G-protein βγ subunits. Trends Cell Biol. **3:** 230–236.

Ito, H., Y. Fukuda, K. Murata and A. Kimura, 1983 Transformation of intact yeast cells treated with alkali cations. J. Bacteriol. **153:** 163–168.

Kao, L.-r., J. Peterson, R. Ji, L. Bender and A. Bender, 1996 Interactions between the ankyrin repreat-containing protein akr1p and the pheromone response pathway in *Saccharomyces cerevisiae*. Mol. Cell. Biol. **16:** 168–178.

Konopka, J. B., D. D. Jenness and L. H. Hartwell, 1988 The C-terminus of the *Saccharomyces cerevisiae* α-pheromone receptor mediates an adaptive response to pheromone. Cell **54:** 609–620.

Kurjan, J., 1992 Pheromone response in yeast. Annu. Rev. Biochem. **61:** 1097–1129.

Lambright, D. G., J. Sondek, A. Bohm, N. P. Skiba, H. E. Hamm *et al.*, 1996 The 2.0 Å crystal structure of a heterotrimeric G protein. Nature **379:** 311–319.

Lee, E., R. Taussig and A. G. Gilman, 1992 The G226A mutant of Gsα highlights the requirement for dissociation of G protein subunits. J. Biol. Chem. **267:** 1212–1218.

Liu, M., and M. I. Simon, 1996 Regulation by cAMP-dependent protein kinease of a G-protein-mediated phopholipase C. Nature **382:** 83–87.

MacKay, V. L., S. K. Welch, M. Y. Insley, T. R. Manney, J. Holley *et al.*, 1988 The *Saccharomyces cerevisiae BAR1* gene encodes an exported protein with homology to pepsin. Proc. Natl. Acad. Sci. USA **85:** 55–59.

Marcus, S., C.-B. Xue, F. Nadier and J. M. Becker, 1991 Degradation of **a**-factor by a *Saccharomyces cerevisiae* α-mating-type specific endopeptidase: evidence for a role in recovery of cells from G_1 arrest. Mol. Cell. Biol. **11:** 1030–1039.

Orr-Weaver, T. L., J. W. Szostak and R. J. Rothstein, 1983 Genetic applications of yeast transformation with linear and gapped plasmids. Methods Enzymol. **101:** 228–245.

Pryciak, P. M., and L. H. Hartwell, 1996 *AKR1* encodes a candidate effector of the $G_{\beta\gamma}$ complex in the *Saccharomyces cerevisiae* pheromone response pathway and contributes to control of both cell shape and signal transduction. Mol. Cell. Biol. **16:** 2614–2626.

Reed, S. I., J. A. Hadwiger and A. T. Lorincz, 1985 Protein kinase activity associted with the product of the yeast cell division cycle gene *CDC28*. Proc. Natl. Acad. Sci. USA **82:** 4055–4059.

Reneke, J. E., K. J. Blumer, W. E. Courchesne and J. Thorner, 1988 The carboxy-terminal segment of the yeast α-factor receptor is a regulatory domain. Cell **55:** 221–234.

Rothstein, R., 1991 Targeting, disruption, replacement, and allele rescue: integrative DNA transformation in yeast. Methods Enzymol. **194:** 281–301.

Sambrook, J., E. F. Fritsch and T. Maniatis, 1989 *Molecular Cloning: A Laboratory Manual.* Cold Spring Harbor Laboratory Press, Cold Spring Harbor, NY.

Schreibmayer, W., C. W. Dessauer, D. Vorobiov, A. G. Gilman, H. A. Lester *et al.*, 1996 Inhibition of an inwardly rectifying K^+ channel by G-protein α-subunits. Nature **380:** 624–627.

Schwartz, R. M., and M. O. Dayhoff, 1979 Atlas of protein sequence and structure. National Biomedical Research Foundation, Washington, DC.

Sherman, F., G. R. Fink and J. B. Hicks, 1986 *Laboratory Course Manual for Methods in Yeast Genetics*. Cold Spring Harbor Laboratory Press, Cold Spring Harbor, NY.

Simon, M.-N., C. D. Virgilio, B. Souza, J. R. Pringle, A. Abo *et al.*, 1995 Role for the Rho-family GTPase Cdc42 in yeast mating-pheromone signal pathway. Nature **376:** 702–705.

Slater, M. R., and E. A. Craig, 1987 Transcriptional regulation of an hsp70 heat shock gene in the yeast *Saccharomyces cerevisiae*. Mol. Cell Biol. **7:** 1906–1916.

Sondek, J., A. Bohm, D. G. Lambright, H. E. Hamm and P. B. Sigler, 1996 Crystal structure of a G_α protein $\beta\gamma$ dimer at 2.1 Å resolution. Nature **379:** 369–374.

Spain, B. H., D. Koo, M. Ramakrishnan, B. Dzudzor and J. Colicelli, 1995 Truncated forms of a novel yeast protein suppress the lethality of a G protein α subunit deficiency by interacting with the β subunit. J. Biol. Chem. **270:** 25435–25444.

Sprague, G. F., and J. W. Thorner, 1992 *Pheromone Response and Signal Transduction during the Mating Process of Saccharomyces cerevisiae*. Cold Spring Harbor Laboratory Press, Cold Spring Harbor, NY.

Stone, D. E., and S. I. Reed, 1990 G protein mutations that alter the pheromone response in *Saccharomyces cerevisiae*. Mol. Cell. Biol. **10:** 4439–4446.

Stone, D. E., G. M. Cole, M. Lopes, M. Goebl and S. I. Reed, 1991 *N*-myristoylation is required for function of the pheromone-responsive G_α protein of yeast: Conditional activation of the pheromone response by a temperature-sensitive *N*-myristoyl transferase. Genes Dev. **5:** 1969–1981.

Stratton, H. F., J. Zhou, S. I. Reed and D. E. Stone, 1996 The mating-specific G_α protein of *Saccharomyces cerevisiae* downregulates the mating signal by a mechanism that is dependent on pheromone and independent of $G_{\beta\gamma}$ sequestration. Mol. Cell. Biol. **16:** 6325–6337.

Tatchell, K., K. A. Nasmyth and B. D. Hall, 1981 In vitro mutation analysis of the mating-type locus in yeast. Cell **27:** 25–35.

Trueheart, J., J. D. Boeke and G. R. Fink, 1987 Two genes required for cell fusion during yeast conjugation: Evidence for a pheromone-induced surface protein. Mol. Cell. Biol. **7:** 2316–2328.

Whiteway, M., I. Hougan, D. Dignard, D. Y. Thomas, L. Bell *et al.*, 1989 The *STE4* and *STE18* genes encode potential β and γ subunits of the mating factor coupled G protein. Cell **56:** 467–477.

Whiteway, M., K. L. Clark, E. Leberer, D. Dignard and D. Y. Thomas, 1994 Genetic identification of residues involved in association of α and β G-protein subunits. Mol. Cell. Biol. **14:** 3223–3229.

Whiteway, M. S., C. Wu, T. Leeuw, K. Clark, A. Fourest-Lieuvin *et al.*, 1995 Association of the yeast pheromone response G protein βγ subunits with the MAP kinase scaffold ste5p. Science **269:** 1572–1574.

Zhao, Z., T. Leung, E. Manser and L. Lim, 1995 Pheromone signalling in *Saccharomyces cerevisiae* requires the small GTP-binding protein Cdc42p and its activator *CDC24*. Mol. Cell. Biol. **15:** 5246–5257.

Communicating editor: M. D. Rose